

# The Superconducting Separated-Orbit Cyclotron TRITRON

U. Trinks, P. Schütz  
Physik Department  
Technische Universität München  
D-85748 Garching, Germany

## I. SUMMARY

The Tritron will be a separated-orbit cyclotron with superconducting channel magnets and superconducting accelerating cavities. The cavities of the reentrant type with prolonged accelerating lips and wedge-shaped gaps will accelerate 20 ion beams in parallel at a frequency of 170 MHz. They are made from copper with a thin PbSn layer as superconductor. Presently all major components of the Tritron are fabricated, more than 60% of them are assembled in the cryostat. Ion beams were injected and transported successfully along the first half turn of the orbit, crossing in total eight channel magnets and three cavities. Completion of the machine is expected for the end of this year.

## II. THE TRITRON CONCEPT

The original concept of a separated-orbit cyclotron was proposed already in 1963 by F.M. Russell [1]. A small experimental SOC was developed then, however it never came into operation [2]. The Tritron will be a separated-orbit cyclotron with superconducting channel magnets and superconducting accelerating cavities [3,4]. The channel magnets are arranged such, that the ions follow a spiral orbit with constant turn separation, given by the width of the channel magnets. The field level in each channel is set independently according to informations from beam position probes. Axial beam displacements can be corrected by small superconducting steerer magnets. Succeeding channels have alternating field gradients, causing strong transverse focusing [5]. Radially neighbouring channel magnets are put together, forming flat sectors. In intermediate gaps between two sectors superconducting rf-cavities of the reentrant type are inserted, operating in the fundamental mode. The accelerating voltage per turn has to be sufficient to provide for a velocity increase of the particles according to the turn separation of the spiral orbit. The system is phase focusing because of the free choice of the field gradients at the separated orbits [6].

Superconductivity is of crucial importance for this concept, first to save dissipation of energy in the magnets and the rf-system. Secondly it makes possible high current density coils and hence small cross sections of the magnet channels and a short range of the stray-fields. This enables one to optimize the cavities with respect to losses and peak fields and to operate them superconducting at all.

The principal impetus for the development of the Tritron has come from the demand for a high current accelerator in the energy range 500 MeV to 1 GeV for the production of intense beams of secondary particles. The isochronous cyclotron is limited to beam currents of 1-2 mA because of the lack of phase focusing and hence poor extraction efficiency. Moreover the strong magnetic stray-fields would prohibit superconducting cavities. The advantages of the Tritron concept compared to a superconducting linear accelerator lie in lower capital and operating costs for the accelerator, buildings and shielding.

Important advantages result from the design of the Tritron cavities. The cavities are made from copper with a thin PbSn-layer as superconductor. The cavities can be handled under real laboratory conditions instead of clean room environment, in spite of the large surface of several m<sup>2</sup> each. The cavities can be operated in the ordinary insulating vacuum of the cryostat, a separated vacuum chamber for the beam is not needed. Cooling is made indirectly by pipes with liquid helium at 4.2 K, which are connected to a reservoir (thermal siphon). No intricate bath cryostat limits the installation of couplers or tuning systems.

The width of the wedge-shaped accelerating gap increases proportional to the radius, so that the transit time factor is a constant for all beam holes. The frequency is rather low due to the large size of the cavities. Therefore the gap width can be made relatively large without loosing at the transit time factor. The geometry factor is about 90.

Each cavity accelerates up to 20 beams in parallel, so that the number of single cavities including their rf-equipment is considerably reduced. The multiple use of the gap and the low frequency cause extremely low dissipated wall losses per voltage gain of the particles. For the existing Tritron-cavities values of less than 1 W/MV were obtained routinely at an amplitude of the accelerating field in the centre of the gap of 6 MV/m. A total voltage of 800 MV would require a cooling power of less than 1 kW at 4.2 K, respectively less than  $\sim 0.5$  MW for the refrigerator plant. These numbers

could be more than one order of magnitude higher for single-beam hole cavities with higher frequency for a proton linear accelerator, even if produced from niobium.

The problem of beam-induced voltages respectively of dissipated energy by higher-order modes in a Tritron cavity by several distributed beams is not yet investigated in detail. The total current seen by the cavities is the beam current multiplied by the number of turns. However the phases of the parallel micro bunches generally are different depending on the beam hole position, so that the effective current will be less. The number of cavities is strongly reduced compared to a linear accelerator with the same total accelerating voltage, so that the total dissipated power from HOM may be even much less. There is easy access to the cavities to install HOM couplers. The rf-frequency over the repetition frequency of the bunches, the harmonic number, is small compared to those in big ring accelerators, which is advantageous too. Finally there are numerous possibilities to control the beam position individually, even the focusing power could be varied.

Therefore the Tritron concept is expected to be a promising candidate for providing high cw-currents of protons or heavy ions up to specific energies of 800 MeV and more in several steps, for example by three successive Tritron rings [4].

### III. THE TRITRON DESIGN

The Tritron presently under construction was designed to fit into the existing laboratory with a MP-tandem as injector (Fig.1). It will increase the ion energies by a factor of 5. It is a rather small machine to develop the superconducting

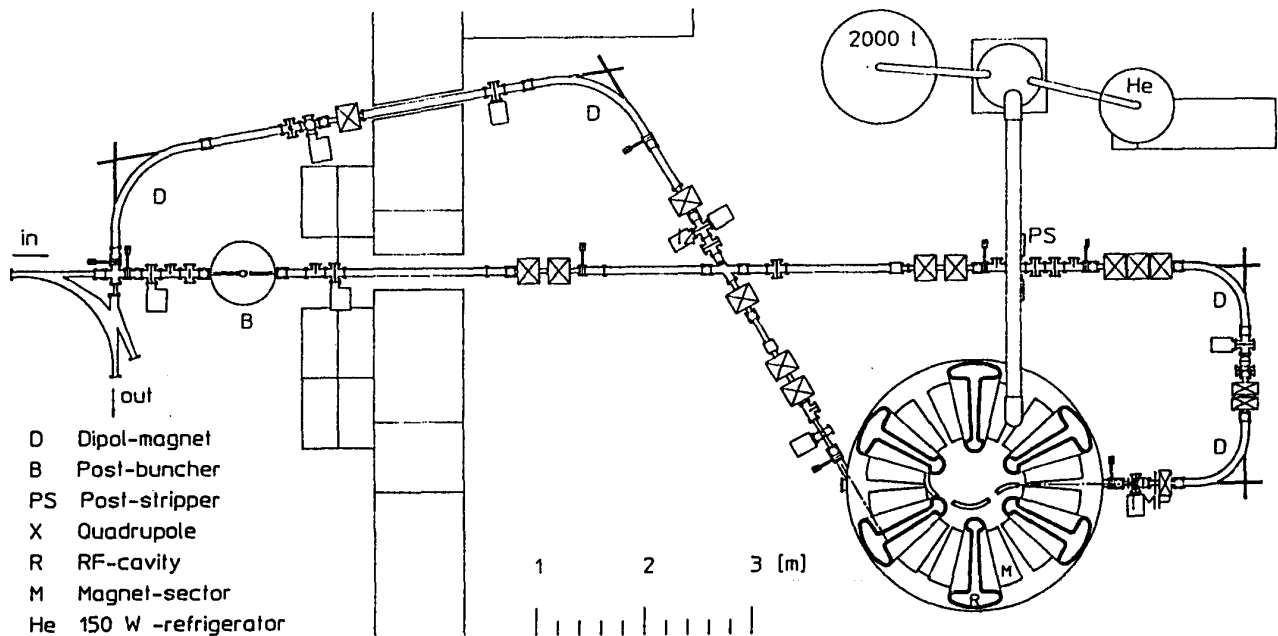


Figure 1: Plan view of the Tritron hall.

components and to provide experience in the design and operation of this new type of accelerator. When the project was started it was unknown, if superconducting cavities of the Tritron type would operate at all. In order to keep the accelerating voltages per turn as low as possible (design: 3.2 MV on the last turn), the turn separation respectively the width of the channel magnets were chosen as small as possible ( $\Delta r = 40$  mm). Due to the rather small aperture of the magnets ( $d = 10$  mm) the machine will not be suited to accelerate beams with very high currents.

### IV. THE MAGNETS

The beam is guided by 238 superferric, independent channel magnets of the window-frame type with alternating gradients along a spiral orbit with almost 20 turns. The spiral consists of  $30^\circ$ -arcs and drift lengths between them. The injection radius is 66 cm, the extraction radius 145 cm. Radially neighbouring channels are joined into 12 flat sectors. All sectors are of equal geometric shape except the last two, where one channel is removed for injection respectively extraction. The bending radius of the innermost channels is  $\rho_1 = 430$  mm, of the outmost  $\rho_{20} = 942$  mm.

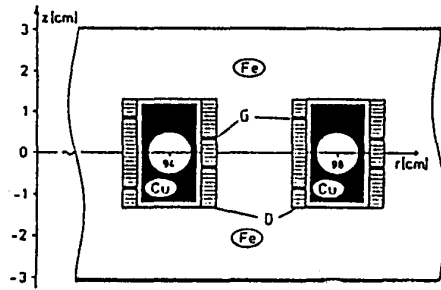


Figure 2: Cross section through a magnet sector with two adjacent channels. G gradient windings, D insulating layers.

Each sector consists of two steel sheets (Fig.2), each 30 mm thick, with curved slots every 4 cm (width 22 mm, depth 15.5 mm). All pieces from steel are Ni plated to avoid rust. The maximum induction is limited by the saturation of the steel to about  $B_{sat} \approx 2$  T. Thus the overall current density in the superconducting coils can be chosen  $\geq 600$  A/mm, and the radial width of the coil can be made small ( $\approx 3$  mm). The coils consist of  $2 \times 13$  windings of a Rutherford-type cable, including a separate gradient winding in each half-coil. The half-coils were wound directly into the slots by a computer controlled winding machine (640 half-coils within 17 months) and then vacuum impregnated with epoxy in situ. A copper profile (with a 10 mm bore for the beam) shields the coil from beam losses. Flat disc springs between the copper profile and the coil prevent the coil from cracking of from the steel.

The injection is made by three superconducting channel magnets. The third one with a bending radius of 300 mm imposes the bending limit for the Tritron. This channel is made from FeCo to obtain up to 2.4 T.

In order to guide the beam along the central orbit the currents of each of the  $(238 + 3)$  channels have to be adjusted individually. The difference between maximum and minimum current of all channels is less than 170 A. All main coils will be connected in series. Each half of a main coil has a superconducting switch with superconducting joints in parallel, which will be turned to the superconducting state as soon as the appropriate current of the coil is achieved. Further variation of the current from the power supply will be shared between the bypass switch and the coil, according to the ratio of the inductances ( $\approx 10^{-3}$ ). The switches are made of superconducting wires (hairpin shape) with the copper matrix etched off along  $\approx 3$  cm, which can be heated above the critical temperature with an Allen-Bradley resistor.

## V. THE CAVITIES

In each second of the intermediate free sectors a superconducting rf-cavity with a radial length of 120 cm is inserted. The accelerating lips are prolonged radially, forming a wedge-shaped gap of 62 mm width at the first beam hole and 128 mm at the last (Fig.3). The accelerating lips are  $\approx 90$  cm long and  $\approx 15$  cm high. The surrounding bulge for the

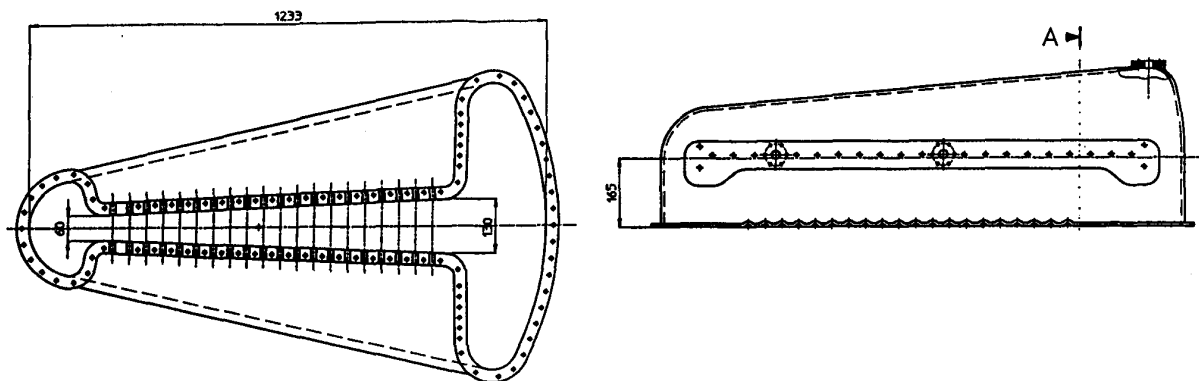


Figure 3: Cross sections of the upper half of a cavity. Numbers in mm.

magnetic rf-flux was chosen as big as possible to keep the surface fields and thus the losses small. All radii of curvature were made sufficiently large to get the electrical peak field not more than 1.5 of the maximum field in the gap. The beam hole diameters are 13 mm, the length of the cutoff bores in the accelerating lips is 30 mm.

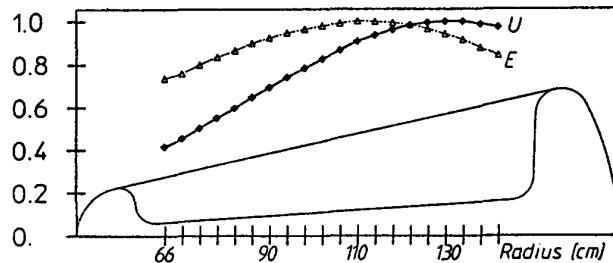


Figure 4: The radial characteristics of the normalized voltage  $U$  and the gap field  $E$ .

The cavities are operated in the fundamental mode at a frequency of  $\nu_{rf} = 170$  MHz. The radial field and voltage characteristics are shown in Fig. 4. The radial increase of the voltage due to that of the gap width corresponds approximately to the requested energy gain of the ions. So far a maximum voltage  $U_{20} = 1.2$  MV was obtained at the last beam hole corresponding to a maximum electrical gap field at the 13<sup>th</sup> hole of 10.6 MV/m and a maximum surface induction of  $\simeq 0.023$  T near to the first beam hole.

In the fundamental mode no currents should cross the horizontal plane of symmetry. Therefore the cavities can be made from two halves, which are connected simply by a flat joint. The cavity halves were fabricated by electroplating copper (for the most parts 10 mm thick) onto fibre-glass shells, which were removed afterwards [7]. The copper halves were electroplated with a  $\simeq 5$   $\mu\text{m}$  thick layer of PbSn (4 Sn, 96 Pb atoms), which has a critical temperature of  $T_c = 7.5$  K. Two O-shaped cooling pipes are attached on both sides of the cavity (thermal siphon). During a test more than 100 W dissipated rf-power was removed without quenching the cavity.

Due to rather small mechanical tolerances the frequencies of the cavities are equal within  $\pm 1.5 \cdot 10^{-4}$ . Tuning is made in three steps: coarse (50 kHz) by mechanical deformation (at A in Fig.3.), fine (300 Hz) by moving sapphire rods into the rf-field volume, and final phase corrections by a fast electronic control system adapted from the S-DALINAC [8]. Sapphire has a low rf-loss factor and high thermal conductivity at low temperature. The frequency shift due to electromagnetic pressure was  $\sim 230$  Hz at a maximum voltage  $U_{20} = 1200$  kV at the last beam hole. Frequency variations due to acoustic vibrations are less than 10 Hz, partially owing to the fact, that the cavities are supported very near to the nodes of the fundamental vibration (frequency:  $\simeq 170$  Hz).

PbSn is a better superconductor than pure Pb because of its enhanced stability against chemical reactions, the lower BCS resistance and better throwing power during the electroplating procedure [9]. The temperature dependent part of the surface resistance is given by

$$R_{BCS} = 6.85 \cdot 10^{-5} \cdot \nu^{1.9} \cdot \frac{1}{T} e^{-\frac{15.1}{T}} \quad (1)$$

with  $R_{BCS}$  in  $\Omega$ ,  $\nu$  in GHz and  $T$  in K. Due to the rather low frequency of 170 MHz the cavity needs not to be cooled down below 5 K. At  $T = 5$  K one has  $R_{BCS} = 2.3 \cdot 10^{-8} \Omega$ , which gives the unloaded quality factor  $Q_o = G/R_{BCS} = 4.1 \cdot 10^9$ , where  $G = 95 \Omega$  is the geometry factor of the cavity. This  $Q_o$ -value represents an upper limit. Additional contributions  $R_{RES}$  to the surface resistance  $R_S$ , which are independent from temperature, e.g. dielectric layers, normal-conducting spots or magnetic flux causing persistent currents will lower the  $Q_o$ -value. The stray fields of the channel magnets and current leads have to be shielded by thin steel sheets below  $\simeq 10^{-4}$ .

In Fig.5 and 6 some measurements of the  $Q_o$ -values versus  $U_{20}$  respectively the maximum gap field  $E_{max}$  at the 13<sup>th</sup> beam hole are shown for two of the cavities. The temperature was below 5 K, the background induction  $\leq 5 \cdot 10^{-5}$  T. The cavities were electroplated with the PbSn-layers in alphabetic order. The improvement of the later  $Q_o$ -values indicates the progress in the surface preparation technique. The curves slope at low voltages slightly, at those above  $\simeq 600$  kV more steeply due to starting field emission. The dotted curves are for constant dissipated heat, 6 W respectively 12 W per cavity. During the first test of cavity C, the maximum gap field was limited by multipacting. The improvement of the third test, compared to the second one, was obtained by extended rf- and He-processing. The quality factor of cavity B showed no degradation during several months (test 1, resp. 2), though the cavities were exposed to air each time, when the vacuum vessel was opened. The third curve was measured two years after the second test in August 93. It shows a degradation of the quality factor at medium and high field levels. After the test a wide spread layer with a certain roughness was found on the cavity surface, which can be easily removed. Further tests are needed.

The insulating vacuum is not separated from the beam vacuum in the Tritron. This good results in spite of the large total surface of  $\simeq 3$  m<sup>2</sup> per cavity can be explained by the fact, that the heat, dissipated in small normal-conducting

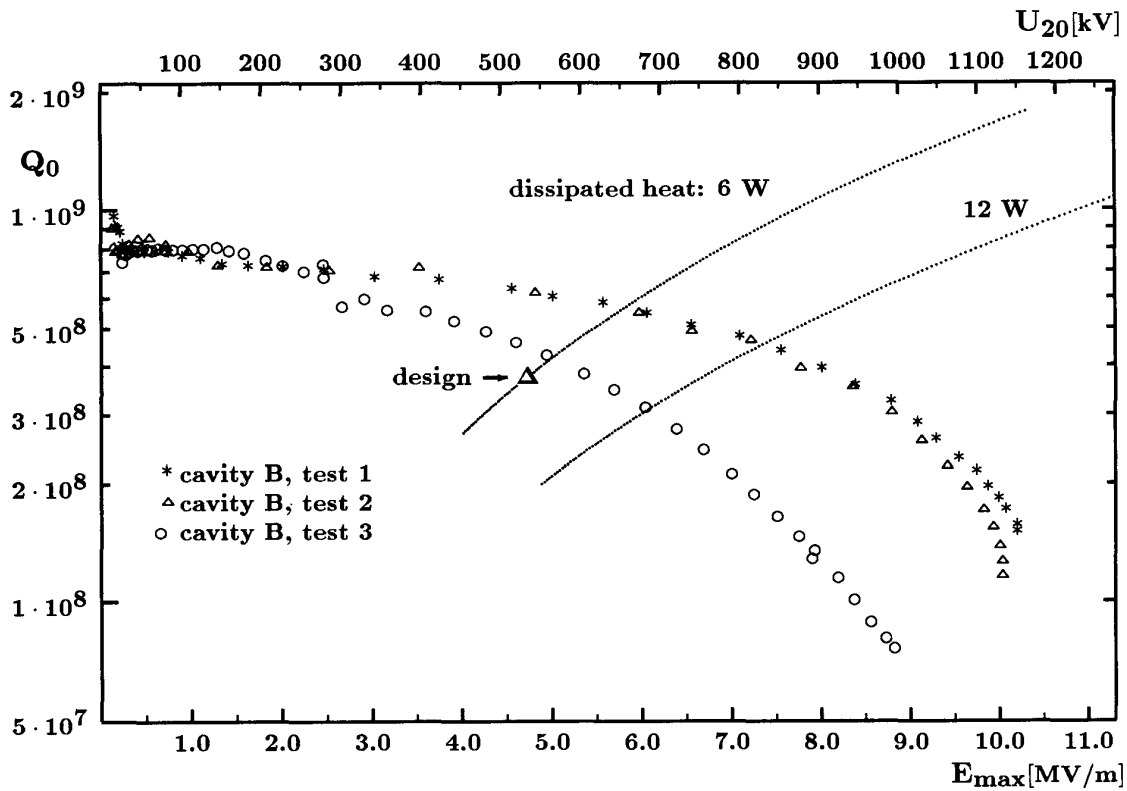


Figure 5: Unloaded quality factor  $Q_0$  of the second Tritron cavity versus the voltage  $U_{20}$  and the maximum gap field.

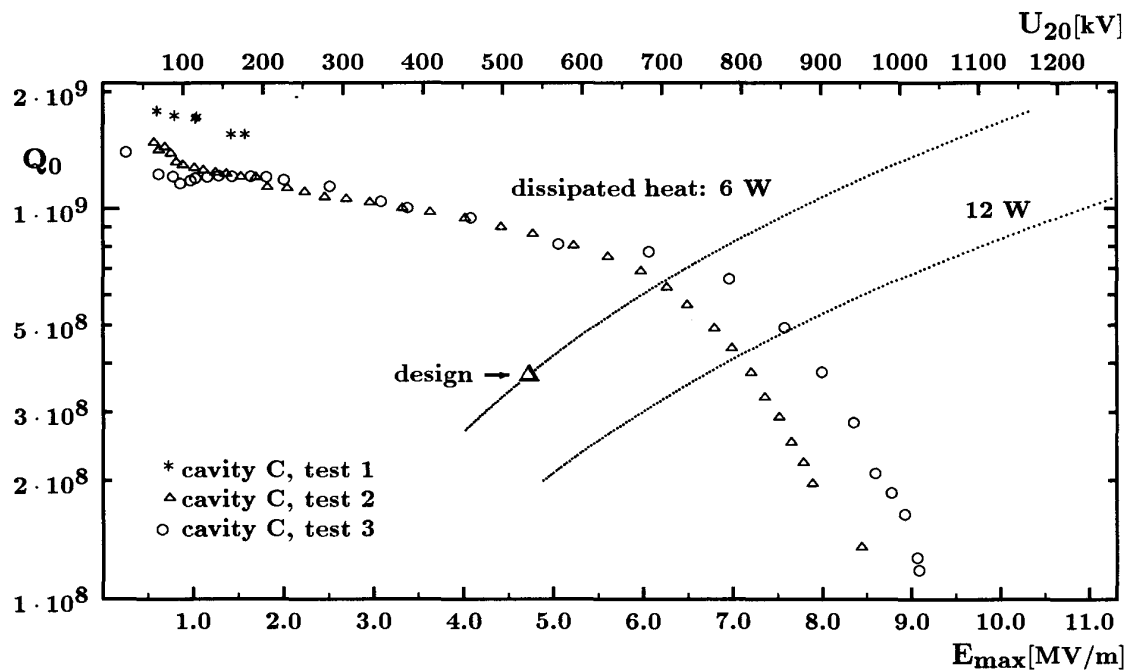


Figure 6: Unloaded quality factor  $Q_0$  of the third Tritron cavity versus the voltage  $U_{20}$  and the maximum gap field.

spots e.g., will be lead away from the thin PbSn layer into the copper body very effectively, causing a rather small temperature increase and preventing the spot to grow, at least below a certain maximum power input. In addition the skin depth of the rf-fields in normal-conducting PbSn exceeds the thickness of the layer considerably.

## VI. PRESENT STATUS

All accelerating cavities and magnet sectors including spare are manufactured and ready for installation. Representative field measurements with good results were made on some 50 channel magnets. Four cavities have been conditioned so far and exceed the design values. The assemblage of all parts inside the vacuum vessel is going on. Each cavity is suspended on a separate platform together with both adjacent magnet sectors and then hung as a unit on the torus-shaped helium reservoir in the vacuum vessel. Up to now four of the six units are ready.

The cryosystem including the refrigerator (155 W at 4.6 K) is operating well. Evacuation of the cryostat needs about 24 h. Cooling down from 300 K to 4.2 K of  $\simeq 40\%$  of the final mass ( $\simeq 6$  tn) is done within 60 h with somewhat reduced refrigerator power. The stand-by load on the 4.5 K level is less than 50 W.

The beam guiding system between the tandem and the Tritron is ready except of the bunching system [10]. The computer control system of the tandem and Tritron is in an advanced state [11].

When the first three units together with the three injection channels were installed, ion beams were injected into the Tritron for the first time (40 MeV  $^{32}\text{S}^{+14}$  and 20 MeV  $^{16}\text{O}^{+8}$ , not yet bunched). The main results of these tests can be summarized as follows:

- First beams passed successfully through the three injection channels, the following five channel magnets as well as three cavities on half of the innermost turn. The beam dimensions correspond to the expected values (diameter some mm). Some optical properties of the magnets were checked with good results.
- No influence of stray-fields on the cavities were observed. When operating the first cavity at rather high levels, the expected horizontal spreading of the unbunched beam was observed downstream.
- In total 122 channel magnets were operating at the same time with currents up to 1000 A (about 60 % of maximum). The technique of individual current setting in the channels by just one power supply by means of the superconducting bypass switches was tested successfully. The fields in the three injection channels and the following five, innermost channels with the switch superconducting stayed stable, when the current in the switches was changed by  $\pm 100$  A. No effect on the beam positions could be observed.
- In total 6 of some 120 beam position probes (wire scanners) were operating under real conditions with good results.
- The first superconducting steerer magnet for axial beam corrections was taken into operation.

## VII. ACKNOWLEDGEMENTS

Thanks are given to all members of the Tritron group. This work was funded by the German Federal Minister for Research and Technology (BMFT) under the contract number 06 TM 189.

## References

- [1] Russell, F.M., "A fixed-frequency, fixed-field, high-energy accelerator", Nucl. Instr. Meth. 23, 229 (1963).
- [2] Martin, J.A., "The separated-orbit cyclotron", IEEE Trans. Nucl. Sci. NS-13, 288 (1966).
- [3] Trinks, U., Assmann, W., Hinderer, G., "The Tritron: A superconducting separated-orbit cyclotron", Nucl. Instr. Meth., A244, 273 (1986).
- [4] Trinks, U., "The superconducting sep.-orbit cyclotron Tritron", 13<sup>th</sup> Int. Conf. on Cyclotrons and their Applications, July 1992, Vancouver, 693.
- [5] Hinderer, G., Rieß, C., Trinks, U., "Transverse beam dynamics and coupling effects in the Tritron", Nucl. Instr. Meth., A317, 13 (1992).
- [6] Trinks, U., "Longitudinal particle dynamics in the Tritron", Nucl. Instr. Meth. A306, 27 (1991).
- [7] Grundey, T., Labedzki, J., Schütz, P., Trinks, U., "The superconducting accelerating cavities for the Tritron", Nucl. Instr. Meth. A306, 21 (1991).
- [8] Aab, V., et al. Proc. European Part. Accel. Conf., 1988, Rome, 335.
- [9] Dietl, L., Trinks, U., "The surface resistance of a superconducting lead-tin alloy", Nucl. Instr. Meth. A284, 293 (1989).
- [10] Hinderer, G., Leu, M., "The beam matching for the tandem-Tritron accelerator system", Nucl. Instr. Meth. A287, 287 (1990).
- [11] Rohrer, L., Schnitter, H., Walchshäusl, B., "The tandem Tritron control system", Nucl. Instr. Meth. A287, 170 (1990).